Journal of Engineering and Technological Sciences

One-dimensional Photonic Crystal with Defects to Detect Gelatine Containing Water

Ary Syahriar[1,*], Nafis Riffat Syahriar[2], Muhamad Giri Suada[3], Kun Mardiwati Rahayu[4], Octarina Nur Samijayani[1], & Ahmad Husin Lubis[1]

[1]Department of Electrical Engineering, Faculty of Science and Engineering, University al Azhar Indonesia, Kompleks Masjid Agung al Azhar, Jalan Sisingamangaraja Blok M. Jakarta 12110, Indonesia
[2]Material Engineering Department, Faculty of Mechanical and Aeronautics Engineering, Bandung Institute of Technology, Jalan Ganesa No. 10, Lebak Siliwangi, Kecamatan Coblong, Kota Bandung, Jawa Barat 40132, Indonesia
[3]Aeronautics Department, Faculty of Mechanical and Aeronautics Engineering, Bandung Institute of Technology, Jalan Ganesa No. 10, Lebak Siliwangi, Kecamatan Coblong, Kota Bandung, Jawa Barat 40132, Indonesia
[4]Department of Biology, Faculty of Science and Engineering, University al Azhar Indonesia, Kompleks Masjid Agung al Azhar, Jalan Sisingamangaraja Blok M. Jakarta 12110, Indonesia

*Corresponding author: ary@uai.ac.id

Abstract

Gelatine is commonly found in food, pharmaceutical, health, and cosmetic products. However, its use has generated significant debate due to concerns about the numerous sources, particularly for religious reasons. For Muslims and Jews, gelatine derived from porcine sources must be avoided, as it is strictly prohibited by religious laws. The detection in these products is important, and this led to the design of an optical biosensor based on a one-dimensional (1D) photonic crystal (PhC) with a defect layer. The aim was to detect the distinctive characteristics of gelatine with high sensitivity. Additionally, the defect layer was placed in the center of the structure, where the gelatine solution was introduced. The designed PhC structure consisted of *N* layers of $(ZnO/SiO_2)^N$/defect/$(ZnO/SiO_2)^N$. The reflectance and transmittance characteristics of the PhC were calculated by using the transfer matrix method (TMM), performed with the MATLAB software. For simplicity, the normal incidence of light on the PhC was assumed to avoid the complexities of oblique angles. Sensor performance was evaluated by calculating sensitivity (S), quality factor (Q), figure of merit (FOM), resolution (RS), and detection limit (LOD). The biosensor achieved an average S, Q, FOM, RS, and LOD of 225.7694 nm/RIU, 2249.413, 806.3185, 0.1332, and 4.13×10^{-5}, respectively. These metrics showed the simple PhC design was a highly sensitive, non-invasive detection platform for monitoring and identifying gelatine-based products that did not meet Halal and Kosher requirements. The novelty of the study centered on the application of a simple 1D PhC with a defect cavity to detect gelatine concentrations in both aqueous and oily solutions, a problem that had not been addressed in detail.

Keywords: *1D PhC with defects; adulteration; biosensors; food; gelatine; halal; kosher; pharmaceutical.*

Introduction

The pursuit of accurate and efficient methods for detecting specific materials has driven significant advancements in optical sensor technology. Meanwhile, of the various technologies explored, photonic crystal (PhC) has evolved as a promising solution due to the unique ability to manipulate and control the flow of light. PhC, initially proposed by Eli Yablonovitch and Sajeev John (1987), is a new type of artificial material featuring a periodic refractive-index modulation in one, two, or three dimensions (Yablonovitch 1987; John 1987; Awasthi, S.K. et al; 2009; Malaviya, U.; Ojha et al 2006). The unique properties of one-dimensional (1D) PhC have enabled the application in numerous photonic and sensing technologies. For example, in optical communications, defect-engineered 1D PhC was employed to actualize ultra-narrow-band filters with excellent spectral selectivity and transmission characteristics (Li et al., 2024; Li, S et al., 2024; Wu et al., 2025). Recent studies have also reported polarization-selective transmission and angle-independent optical responses in engineered 1D PhC structures. These studies further outlined the potential for polarization management and integrated photonic devices (Wu et al., 2022; Wei et al., 2025). Beyond the diverse photonic applications, 1D PhC has been widely investigated for agriculture, medical diagnostics, pharmaceuticals, food safety monitoring (Li, et al. 2023; Soltani, et al. 2023; Liu, et al 2022; Wang, et al. 2014; Zaky, et al. 2022; Al-Dossari, et al. 2022; Taya., et al. 2022;

ISSN: 2337-5779
DOI: 10.5614/j.eng.technol.sci.2026.58.5.4

DOI: 10.5614/j.eng.technol.sci.2026.58.5.4

Kaviani, 2022; Bazian 2021) optical switching (Zheng, S., et al 2021), biosensing (Suthar, 2021; Aly, et al. 2021; Abadla, et al 2022a), and aerospace sensing (Kirubel, 2020; Mao, et al. 2024).

Recent advances in photonic biosensing outlined the convergence of integration, intelligence, multiplexing, and flexibility. Lab-on-chip integration has been enhanced by microfluidic–photonic hybrid platforms. This included monolithic silicon photonic circuits and flexible paper-based plasmonic microfluidics for multiplexed diagnostics (Zhang et al., 2019) and wearable sweat analysis, respectively (Li et al., 2024). Additionally, artificial intelligence has also become central, with machine learning enhancing signal processing and analyte discrimination. Aalizadeh et al. (2024) showed that multi-resonance biosensors combined with machine learning (ML) algorithms significantly improved detection accuracy. Multiplexed detection is enabled by PhC and plasmonic architectures, such as quasi-crystal fiber plasmonic biosensors and hydrogel–plasmonic hybrids for viral sensing (Sharma et al., 2022) and protein analysis (Tan et al., 2015), respectively. Finally, flexible and wearable photonic devices are materializing for continuous monitoring, ranging from plasmonic paper-based microfluidics (Li et al., 2024) to hydrogel-based thin-film lasers for on-skin sensing (Wang et al., 2024). These developments collectively outline the growing versatility and clinical potential of photonic biosensors. Sensing capabilities are in high demand, particularly in biomedical science and engineering, where affordability, ease of use, and precision are crucial. Moreover, 1D PhC with engineered defect layers offered adjustable optical responses. This prompted the development of cost-effective, user-friendly photonic biosensors, specifically designed to detect gelatine.

Gelatine refers to a protein obtained by partially hydrolyzing collagen from animal skin and bones. This protein is characterized by gelation, emulsification, and stabilization properties, which play a crucial role in food and pharmaceutical applications. Gelatine is extracted from porcine or bovine sources, which are cost-effective. In the food industry, this protein serves as a gelling agent in desserts and dairy products, while in pharmaceuticals, gelatine is widely used to manufacture capsules, including dietary supplements. The global market, driven by strong demand from the food, pharmaceutical, and biomedical sectors, produces roughly 326,000 tons annually valued at approximately USD 3.6 billion, and is projected to reach USD 6.7 billion by 2027. Prior studies reported that of this output, 46 %, 29.4 %, 24 %, and ~2 % was derived from porcine skin, bovine sources, a mix of bovine and porcine bones, and alternative sources such as donkey, horse hide, and fish skin, respectively (Hassan, et al. 2024; Schrieber, 2007; Thomas, 2023; Alipala, et al, 2021; Uddin et al, 2021). Gelatine from porcine is preferred over the bovine counterpart due to the greater availability of pig-derived raw materials. This also included concerns over bovine spongiform encephalopathy (BSE), or "mad cow disease" (Hassan et al. 2024; Schrieber, 2007; Thomas, 2023; Alipala, 2021).

The extraction from porcine tended to dominate the global market, resulting in its widespread use in commercial food, pharmaceutical, and cosmetic products, many of which are religiously or culturally prohibited in certain communities. Most food or pharmaceutical products containing porcine-derived gelatine are strictly forbidden for consumption by both Muslims and Jews. As a result, several studies and industries tend to develop alternative sources that meet the dietary and religious requirements of Halal and Kosher consumers. Fish is a recently discovered alternative source of gelatine, considering the religious restrictions and health concerns associated with porcine and bovine. The growing production of gelatine extracted from fish is also driven by increasing demand from Halal and Kosher food consumers. Its use in the food industry is limited by several challenges, including undesirable properties, namely poor texture, dark color, and unpleasant odor (Thomas 2023; Uddin, 2021). Additionally, concerns over fraud and mislabeling have heightened consumer awareness alongside skepticism. The accurate detection and identification of gelatine source has become crucial in the modern Halal and Kosher food industries.

Several methods have been developed to detect the origin of gelatine, initially the process depended on two main types. This included chromatographic methods based on amino acid composition and functional group methods, such as Fourier transform infrared spectroscopy (FTIR). However, both methods faced limitations, considering the inability to differentiate gelatine in food mixtures or pharmaceutical products due to the similar chemical compositions of different sources. Other analytical methods have since been developed, including polymerase chain reaction (PCR), spectroscopy, sensors, liquid chromatography-tandem mass spectrometry (LC-MS/MS), and enzyme-linked immunosorbent assays (ELISA) using DNA, peptide, or protein markers. Among these, FTIR has lower sensitivity, demanding extremely pure samples. ELISA, mass spectrometry, PCR, and plasmon resonance biosensors can detect gelatine sources in various food samples. Mass spectrometry is highly sensitivity as well as frequently used to identify adulteration from different sources. However, these current methods are complex and expensive for use in the food industry (Chaudhary et al. 2022).

The present study, driven by the exceptional sensing capabilities of 1D PhC with defects, explored potential methods for efficiently detecting gelatine in water at varying concentrations. This theoretical study further focused on simulating

PhC detection of gelatine in aqueous solution (Aliotta et al 1996). However, the proposed design was readily extended to accommodate gelatine from other sources.

Materials and Methods

Theory and Design of 1D Photonic Crystals Biosensor

In this section, the structure of 1D PhC was described with a defect cavity, including a mathematical model used to evaluate the optical response. The proposed 1D defective PhC biosensor, shown schematically in Figure 1, was designed to detect varying gelatin concentrations in water. A single defect layer was sandwiched between two identical stacks of ZnO/SiO_2 bilayers, producing an overall structure of $(ZnO/SiO_2)^N$/defect/$(ZnO/SiO_2)^N$. The different colours used in the diagram represent the various layers of the structure, with thicknesses denoted as d_1, d_2, and d_D corresponding to ZnO, SiO_2, and the defect. The theoretical simulation was carried out using MATLAB software, with the thicknesses of the ZnO and SiO_2 layers determined using Bragg's law. In this context, the law ensured the photonic bandgap appeared at a wavelength that maximized constructive interference. The defect thickness can be obtained, assuming the normal incidence of the incoming light is given in Eq. (1) (Born & Wolf, 1999; Nguyen, 2020).

$$d_j = \frac{\lambda_{\text{Brg}}}{4n_j} \tag{1}$$

Where j represents the j^{th} layer, and λ_{Brg} is the Bragg wavelength. The width of the defect, denoted as d_D is defined as $d_{\text{D}} = d_1 + d_2$. The central defect cavity with thickness d_D served as a sample chamber for loading different test media. In the simulations, the cavity was filled with aqueous gelatine solutions at varying concentrations (Aliotta F., et al. 1996). Furthermore, the refractive indices of ZnO and SiO_2 were taken as 1.9888 and 1.457, respectively, at a wavelength of 633 nm (Bond et al., 1965; Malitson, 1965). The design used N=9 ZnO/SiO_2 bilayer periods on each side and was illuminated with normally incident light (Nguyen, 2020; Aly A.H., et al. 2023). The number of bilayers (N = 9 on each side) was selected after testing different N values. Fewer layers produced weak band gaps, and several layers increased fabrication complexity with slight performance gain. Therefore, N = 9 offered the best trade-off between sensitivity, resonance sharpness, and practical manufacturability. Wavelengths within the ranges of 540 nm and 760 nm, detected in the visible spectrum of electromagnetic radiation, were used.

The ZnO/SiO_2 bilayers of the 1D defect PhC biosensor were fabricated using a variety of thin-film deposition methods, including sputtering, spin-coating, atomic layer deposition (ALD), and chemical vapor deposition (CVD) (Shen et al., 2016). The two PhC stacks were fabricated either sequentially on a single substrate with a defined spacer defect region, or separately on dual transparent substrates that were united to form the defect cavity (Aly et al., 2023). The defect layer was designed as a microcavity, which was filled through microfluidic injection and sealed (e.g., with PDMS bonding) to confine the aqueous gelatine solution (Mejia-Salazar et al., 2020; Li et al., 2024). This ensured the analyte was localized only in the defect layer while maintaining the structural and optical integrity of the PhC biosensor.

Figure 1

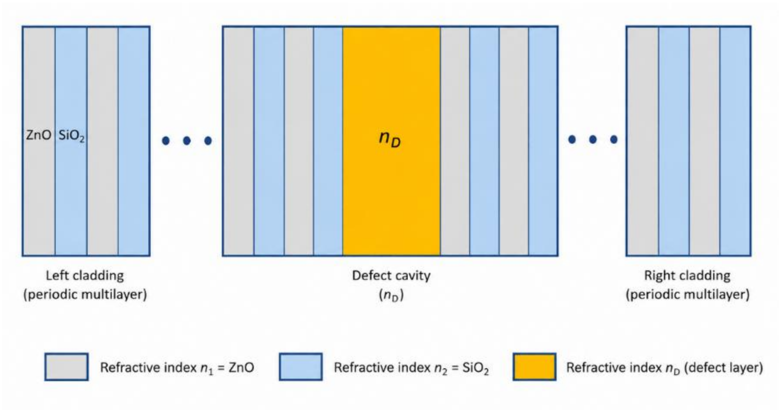

Photonic crystal structure with a defect to detect gelatine containing water emulsion.

The interaction between the electromagnetic field and structure, namely reflection, transmission, and absorption, is calculated by using the widely recognized transfer matrix method (TMM). Furthermore, the material structure used in the simulation is assumed to be homogeneous, isotropic, and non-magnetic. The continuity condition at the interface between each material has been used to calculate the electric and magnetic fields. The matrix form is used to relate the electric and magnetic fields across each layer. For normal incidence, the overall optical response of the multilayer

DOI: 10.5614/j.eng.technol.sci.2026.58.5.4

structure can be described by the total transfer matrix given in Eq. (2) (El-Aziz et al., 2016; Yeh, 2005; Aly et al., 2021; Ashour et al., 2021; Abadla, 2021; Aly, 2022a; Saini, 2023).:

$$M = \prod_{j=1}^{m} M_j = M_1 M_2 M_3 \dots \dots M_m = \begin{bmatrix} M_{11} & M_{12} \\ M_{21} & M_{22} \end{bmatrix} \quad (2)$$

The transfer matrix describing the propagation of the electromagnetic fields through each multilayer structure is expressed in Eq. (3):

$$M_j = \begin{bmatrix} \cos\theta_j & \frac{i\sin\theta_j}{p_j} \\ -ip_j \sin\theta_j & \cos\theta_j \end{bmatrix} \quad (3)$$

Where $\theta_j = \frac{2\pi n_j d_j}{\lambda}$, in this case n_j is the refractive index of j^{th} layer, and d_j represents the width of the j^{th} layer, and λ denotes the wavelength. For the TE mode, the value of $p_j = n_j$. The reflection and transmission coefficients for the proposed design are expressed in Eq (4):

$$r = \frac{M_{21}}{M_{11}}, t = \frac{1}{M_{11}} \quad (4)$$

Therefore, the reflectance (*R*) and transmittance (*T*) of the structure are determined as in Eq (5):

$$R = |r|^2 = \left|\frac{M_{21}}{M_{11}}\right|^2, T = |t|^2 = \left|\frac{1}{M_{11}}\right|^2 \quad (5)$$

The performance of the biosensor was evaluated by considering several metrics, such as sensitivity (*S*), quality factor (*Q*), figure of merit (*FOM*), resolution (*RS*), and detection limit (*LOD*) (Aly et al 2022a; Saini et al 2023; Mejia-Salazar et al. 2020; Gandhi et al 2021). Additionally, the equations for these parameters are shown in Table 1.

Table 1 Equations for Evaluating Biosensor Performances

Parameters	Equation	Definition
Sensitivity (S)	$S = \frac{\Delta\lambda_R}{\Delta n_{gelatin}}$	Sensitivity (*S*) is defined as the shift in the resonance-peak wavelength per unit change in the refractive index
Q Factor	$Q = \frac{\lambda_R}{FWHM}$	*Q* factors explain the sharpness of resonance peaks.
Figure of merit (*FOM*)	$FOM = \frac{S}{FWHM}$	*FOM* is the ability of a biosensor to analyse the change in the resonance peak
Resolution (*RS*)	$RS = \frac{2(FWHM)}{3SNR^{\frac{1}{4}}}$	Small central wavelength changes of defect modes
Limit of Detection (*LOD*)	$LOD = \frac{\lambda_R}{20\,SQ}$	The change of the smallest refractive index that can be measured by the sensor configuration

The present study investigated how varying gelatine concentrations affected the refractive index of both water- and oil-soluble formulations. The parameters used in the calculations are summarized in Table 2, based on data from previous studies (Aliotta, et al 1996).

Table 2 Refractive indices of gelatine containing water and micro emulsions at various concentrations.

Gel Overall (%)	Refractive Index (*n*)
0	1.3864
0.792	1.3872
2.533	1.3887
3.864	1.3901
7.390	1.3942
8.578	1.3957
9.515	1.3964
11.35	1.3976
12.44	1.3983

As shown in Table 2, the refractive index increased monotonically with gelatine concentration. This showed that a direct correlation existed between solute content and optical density of the medium. The nearly linear trend suggested that refractive index variation served as a reliable optical proxy for the concentration. This property is crucial for PhC biosensing, given that small refractive index changes within the defect layer led to measurable shifts in the resonance wavelength. Furthermore, the narrow range of refractive indices (1.3864–1.3983) outlined the need for a high-resolution sensing platform capable of detecting sub-0.001 RIU variations.

Results

The design principles and transfer matrix formalism outlined are the basis for the numerical simulations. In the following section, the results of the diverse simulations were presented, outlining how variations in gelatine concentration within the defect cavity influenced the resonance behavior, including the main performance metrics of the proposed biosensor. The transfer-matrix method outlined above was applied to the defective 1D PhC shown in Figure 1. MATLAB was used to compute the reflectance and transmittance of the design over the visible spectrum range (540–760 nm). Figure 2 shows the comparison of the optical transmittance and the wavelength for the biosensor at various concentrations in the defect layer.

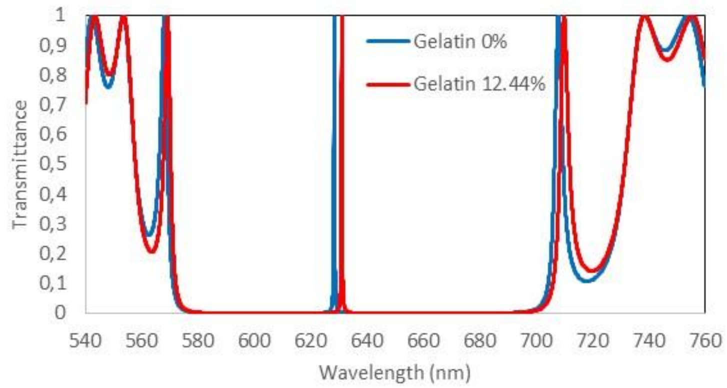

Figure 2

Transmittance characteristics as a function of wavelength under normal incidence for the proposed PhC with a defect layer, at gelatine concentrations of 0% and 12.44%.

Figure 2 shows the transmittance spectra of the 1D PhC at gelatine concentrations of 0% and 12.44% within the defect layer. A distinct resonance peak was observed near the Bragg wavelength, corresponding to the defect mode of the structure. Meanwhile, the PhC effectively suppressed light propagation across the 580–760 nm range, with transmission permitted only at the defect mode. The narrow full width at half maximum (FWHM) of this resonance outlined the precision and high performance of the proposed PhC biosensor.

Figure 3

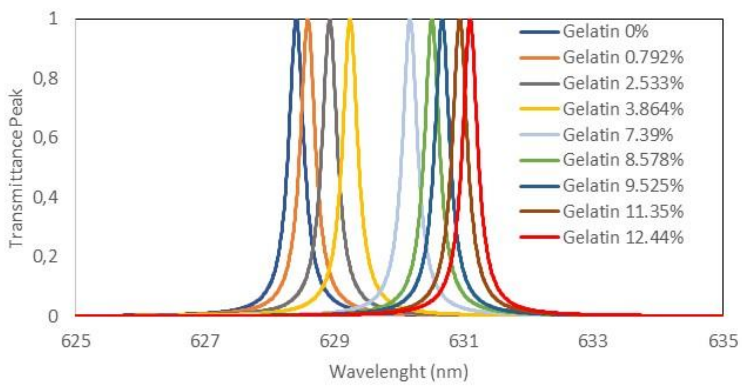

Transmittance as a function of resonant wavelength at different gelatine concentration.

In Figure 3, the variation of the transmittance peak was denoted as a function of wavelength for different gelatine concentrations introduced into the defect layer. For clarity, each curve was color-coded, with blue and red representing the baseline case of 0% gelatine and the highest concentration examined, respectively. A clear trend was observed as the gelatine concentration increased, the defect mode underwent a progressive red-shift, accompanied by subtle changes in transmittance intensity. This behavior arose from the increase in the refractive index of the defect layer with

DOI: 10.5614/j.eng.technol.sci.2026.58.5.4

higher gelatine content, altering the optical path length as well as shifting the resonance condition of the cavity. The systematic displacement of the defect modes confirmed the strong sensitivity of the proposed PhC structure to small concentration variations, thereby showing its suitability for quantitative gelatine detection.

As the gelatine concentration increases, the resonance peak within the PhC tends to shift toward longer wavelengths. This effect was driven by the rising refractive index of the gelatine solution while the defect layer thickness remains fixed. Figure 4 shows the wavelength shift against gelatine concentration for a 900 nm defect layer. Linear regression also showed a strong, nearly linear correlation between gelatine concentration and resonance-peak displacement. The tracking of this shift enabled the proposed biosensor to accurately quantify concentration changes.

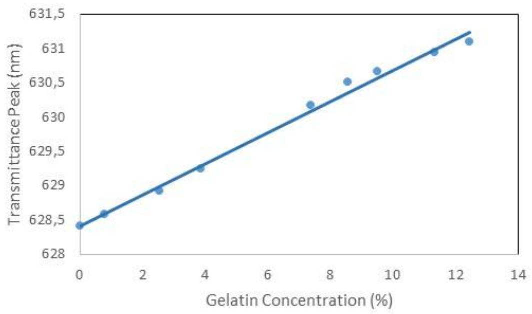

Figure 4 The relation between resonant wavelength changes as a function gelatine refractive index.

The resonance wavelength varied linearly with the gelatine concentration. The relationship between the resonance wavelength and change in concentration was expressed using least squares fitting, as stated in the Eq. (6) below:

$$\lambda_{\mathrm{R}} = 0.2271\ GC + 628.41 \quad (6)$$

where λ_R is the resonance wavelength (nm), and *GC* denotes the gelatine concentration (%). The slope of 0.2271 nm/% shows that each 1% increase in concentration induced a measurable redshift of approximately 0.23 nm in the resonance wavelength. This high degree of linearity confirmed that the sensor response was predictable and suitable for quantitative analysis of gelatine content. Moreover, the small intercept deviation (628.41 nm at 0% gelatine) is consistent with the designed defect-mode position, validating the accuracy of the simulation model. This linear calibration curve enabled the direct conversion of optical measurements into concentration values, particularly valuable for practical applications in food authentication and pharmaceutical quality control.

Discussion

The spectral shifts depict the qualitative response of the sensor to changes in gelatine concentration. This led to the quantitative evaluation of S, Q factor, FOM, and LOD*,* thereby providing deeper insight into the performance of the biosensor. The diverse parameters were summarized to show the efficiency and competitiveness of the proposed design. Table 3 shows the performance calculations of the proposed structure. The average S, average Q factor, FOM, RS, and average LOD are 225.7694 nm/RIU, 2249.413, 806.3185, 0.133193, and 0.00004134, respectively. Based on the high average values of S, Q factor, *FOM*, RS, and detection limit, the biosensor design showed strong potential for efficient gelatine detection in aqueous solutions.

Table 3 Summary of the Performance Calculation on the Proposed Photonic Crystal Biosensor.

Gelatin %	*Wavelength (nm)*	*RI*	*FWHM (nm)*	*Sensitivity (nm/RIU)*	*Q*	*FOM*	*RS*	*LOD*
0	628.405	1.3864	0.28		2244.304			
0.792	628.585	1.3872	0.28	225	2244.946	803.5714	0.208467402	0.00004148
2.533	628.925	1.3887	0.28	226.087	2246.161	807.4534	0.15990257	0.00004128
3.864	629.24	1.3901	0.28	225.6757	2247.286	805.9846	0.142047849	0.00004136
7.39	630.165	1.3942	0.28	225.641	2250.589	805.8608	0.117890311	0.00004136
8.578	630.505	1.3957	0.28	225.8065	2251.804	806.4516	0.112798015	0.00004133
9.515	630.665	1.3964	0.28	226	2252.375	807.1429	0.110746286	0.00004130
11.35	630.935	1.3976	0.28	225.8929	2253.339	806.7602	0.107665398	0.00004132
12.44	631.095	1.3983	0.28	226.0504	2253.911	807.3229	0.106027424	0.00004129

Recent reports on PhC-based biosensors showed a wide range of performance depending on the device architecture, resonance sharpness, and fabrication complexity. For example, two-dimensional (2D) PhC cavity sensors designed for cancer-cell detection showed extremely high sensitivity (≈915.8 nm/RIU) with low detection limits on the order of 10^{-4} RIU (Yang et al., 2023). Photonic-crystal fiber (PCF) designs with plasmonic modes have achieved extremely large numerical sensitivities (~1.3×10^{5} nm/RIU), but these values were typically constrained to narrow refractive-index ranges, requiring sophisticated fabrication processes (Mahfuz et al., 2024). Optimized ternary 1D PhC also reported sensitivities above 690 nm/RIU with high figures of merit (*FOM* ≈ 2561 RIU^{-1}). This outlined the role of structural optimization in narrowing resonance linewidths (Kaviani, 2022). Recently, the engineered eye-shaped 2D cavities achieved sensitivities near 800 nm/RIU with high *Q*-factors (~9.9×10^{3}) and FOM exceeding 4500 RIU^{-1} (Rizk et al., 2025). When compared with the state-of-the-art devices, the designed ZnO/SiO_2 1D defect PhC biosensor showed a moderate sensitivity of ≈225.8 nm/RIU. However, it offered clear advantages in fabrication simplicity, robustness, and direct compatibility with aqueous/oily gelatine samples. Considering the possibility of ultra-high sensitivities in specialized architectures, this design prioritized manufacturability, spectral stability, and application-specific integration, critical for practical deployment in food-safety biosensing.

Conclusion

In conclusion, this study has proven the effectiveness of a 1D PhC biosensor with defects for detecting the characteristics of gelatine-containing water- and oil-soluble solutions. The MATLAB software was used to conduct numerical analysis of the transmittance spectra. This was achieved using the TMM, with normal light incidence on the PhC across varying gelatine concentrations. The results of the simulation showed that with N=9 and a defect width of 900 nm, the biosensor achieved an average S, Q, FOM, RS, and LOD of 225.7694 nm/RIU, 2249.413, 806.3185, 0.1332, and 4.13×10^{-5}, respectively. The results showed that the proposed design held strong potential for gelatine sensing applications. The significance of this study centered on proving that a structurally simple but highly optimized 1D PhC served as a sensitive and practical platform for gelatine-in-solution detection, with direct implications for food authentication, including Halal/Kosher compliance. This capability could be beneficial for Halal and Kosher food consumers, considering the provision of direct, real-time, and accurate analysis to enhance confidence.

Acknowledgments

The authors would like to acknowledge the financial support from the Ministry of Higher Education, Science, and Technology under the 2024 Fundamental Research Grant, as well as from Universitas Al Azhar Indonesia.

Compliance with ethics guidelines

The authors declare they have no conflict of interest or financial conflicts to disclose.

This article contains no studies with human or animal subjects performed by the authors.

References

Abadla, M. M., & Elsayed, H. A. (2020). Detection and sensing of hemoglobin using one-dimensional binary photonic crystals comprising a defect layer. *Applied Optics, 59*(2), 418–424.

Aalizadeh, M., Azmoudeh Afshar, M., Fan, X., et al. (2024). Machine-learning enabled multidimensional data utilization in multi-resonance biosensors: A pathway to enhanced accuracy. Preprint. https://arxiv.org/abs/2412.20245

Aliotta, F., Arcoleo, V., & Turco Liveri, M. L. G. (1996). Structural and dynamical investigation of gelatin containing water-in-oil microemulsions. *Colloid and Polymer Science, 274*, 989–994.

Alipala, J., Mohd Pu'ad, N. A. S., Lee, T. C., Nayan, N. H. M., Sahari, N., Basri, H., Idris, M. I., & Abdullah, H. Z. (2021). A review of gelatin: Properties, sources, process, applications, and commercialization. *Materials Today: Proceedings, 42*, 240–250.

Al-Dossari, M., Awasthi, S. K., Mohamed, A. M., Abd El-Gawaad, N. S., Sabra, W., & Aly, A. H. (2022). Bio-alcohol sensor based on one-dimensional photonic crystals for detection of organic materials in wastewater. *Materials, 15*, 4012.

Aly, A. H., Awasthi, S. K., Mohamed, A. M., Matar, Z. S., Mohaseb, M. A., Al-Dossari, M., Tammam, M. T., Zaky, Z. A., Amin, A. F., & Sabra, W. (2021). Detection of reproductive hormones in females by using 1D photonic crystal-based simple reconfigurable biosensing design. *Crystals, 11*, 1012.

Aly, A. H., Awasthi, S. K., Mohamed, D., Matar, Z. S., Al-Dossari, M., & Amin, A. F. (2021). Study on a one-dimensional defective photonic crystal suitable for organic compound sensing applications. *RSC Advances, 11*, 27115–27122.

DOI: 10.5614/j.eng.technol.sci.2026.58.5.4

Aly, A. H., Awasthi, S. K., Mohaseb, M. A., Matar, Z. S., & Amin, A. F. (2022a). MATLAB simulation-based theoretical study for detection of a wide range of pathogens using 1D defective photonic structure. *Crystals, 11*, 1208.

Aly, A. H., Awasthi, S. K., Mohaseb, M. A., Matar, Z. S., & Amin, A. F. (2022b). MATLAB simulation-based theoretical study for detection of a wide range of pathogens using 1D defective photonic structure. *Crystals, 12*, 220.

Aly, A. H., Mohamed, D., Zaky, Z. A., Matar, Z. S., El-Gawaad, N. S. A., Shalaby, A. S., Tayeboun, F., & Mohaseb, M. (2021). Novel biosensor detection of tuberculosis based on photonic band gap materials. *Materials Research Express, 8*, 085401.

Aly, A. H., Mohamed, B. A., Al-Dossari, M., & Mohamed, D. (2023). A temperature sensor based on Si/PS/SiO_2 photonic crystals. *Scientific Reports, 13*, 21560.

Ashour, H. S., Abohassan, K. M., & Abadla, M. M. (2021). Defective 1D quinary photonic crystal sensors for the detection of cancerous blood cells. *Optical Engineering, 60*(6), 127106.

Awasthi, S. K., Mishra, A., Malaviya, U., & Ojha, S. (2009). Wave propagation in a one-dimensional photonic crystal with metamaterial. *Solid State Communications, 149*, 1379–1383.

Bazian, M. (2021). Photonic crystal add–drop filter: A review on principles and applications. *Photonic Network Communications, 41,* 57–77.

Bond, W. L. (1965). Measurement of the refractive indices of several crystals. *Journal of Applied Physics, 36*(5), 1674–1677

Born, M., & Wolf, E. (1999). Principles of optics: Electromagnetic theory of propagation, interference and diffraction of light (7^{th} ed.). Cambridge University Press.

Chaudhary, V., Kumar, M., Kumar, V., Sharma, S., Dhumal, S., & Maerescu, C. M. (2022). Spectroscopic techniques for authentication of animal origin foods. *Frontiers in Nutrition, 9*, 979205.

El-Aziz, O. A. A., Elsayed, H. A., & Sayed, M. I. (2016). One-dimensional defective photonic crystals for the sensing and detection of protein. *Applied Optics, 55*(29), 8309–8315.

Gandhi, S., Awasthi, S. K., & Aly, A. H. (2021). Biophotonic sensor design using a 1D defective annular photonic crystal for the detection of creatinine concentration in blood serum. *RSC Advances, 11*, 26655–26665.

Hassan, M., Hussain, D., Kawal, T., Xiao, H. M., & Musharraf, S. G. (2024). Method for detection and quantification of gelatin from different sources. *Food Chemistry, 438*, 137970.

John, S. (1987). Strong localization of photons in certain disordered dielectric superlattices. *Physical Review Letters, 58*, 2486–2489.

Kaviani, H., & Barvestani, J. (2022). Photonic crystal based biosensor with the irregular defect for detection of blood plasma. *Optik, 250*, 168109.

Kirubel, A., & Palani, S. (2020). A review on photonics and its applications. *Materials Today: Proceedings, 33,* 3372–3377.

Li, S., Feng, G., Liu, Y., Wu, M., Zhao, X., Sun, F., Gan, Z., Chen, Z., & Yang, Y. (2024). Omnidirectional near-infrared narrowband filters based on defective mirror-symmetry one-dimensional photonic crystals containing hyperbolic metamaterials. *Optical and Laser Engineering, 176*, 108107.

Li, T., Liu, G., Kong, H., Yang, G., Wei, G., & Zhou, X. (2023). Recent advances in photonic crystal-based sensors. *Coordination Chemistry Reviews, 475*, 214909.

Li, Y., Guo, Y., Chen, H., et al. (2024). Flexible wearable plasmonic paper-based microfluidics with expandable channel and adjustable flow rate for portable surface-enhanced Raman scattering sweat sensing. *ACS Photonics, 11*(2), 613–625.

Liu, R., Cai, Z., Zhang, Q., Yuan, H., Zhang, G., & Yang, D. (2022). Colorimetric two-dimensional photonic crystal biosensors for label-free detection of hydrogen peroxide. *Sensors and Actuators B: Chemical, 354*, 131211.

Mahfuz, M. A., Afroj, S., Hossain, M. A., Hossain, M. A., Rahman, A., & Habib, M. S. (2024). An ultra-sensitive visible–IR range fiber-based plasmonic refractive index sensor (arXiv:2401.10968). arXiv.

Mao, D., Chang, L., Lee, D., Yu, A. W., Maruca, B. A., Ullah, K., Matthaeus, W. K., Krainak, M. A., Dong, P., & Gu, T. (2024). Space-qualifying silicon photonic modulators and circuits. *Science Advances, 10*, eead9171.

Malaviya, U., & Ojha, S. P. (2006). Enhancement of omnidirectional total-reflection wavelength range by using one-dimensional ternary photonic bandgap material. *Journal of the Optical Society of America B, 23*, 2566–2571.

Mejia-Salazar, J. R., Cruz, K. R., Vasques, E. M. M., & de Oliveira, O. N., Jr. (2020). Microfluidic point-of-care devices: New trends and future prospects for e-health diagnostics. *Sensors, 20*, 1951.

Nguyen. D.T (2020), Modelling and design photonics by examples using MATLAB®, IOP Publishing Ltd.

Rizk, S., El-Naggar, A. M., Ahmed, A. M., Mehaney, A., Elsayed, H. A., & Aly, A. H. (2025). Photonic crystal biosensor featuring an eye-shaped cavity for precise identification of cancerous cells. *Scientific Reports, 15*, 21987.

Saini, S. K., & Awasthi, S. K. (2023). Sensing and detection capabilities of one-dimensional defective photonic crystal suitable for malaria infection diagnosis from preliminary to advanced stage: Theoretical study. *Crystals, 13,* 128.

Schrieber, H., & Gareis, H. (2007). Gelatine handbook: Theory and practice. Wiley-VCH.

Sharma, A., Singh, S., Mishra, A., et al. (2022). Photonic quasi-crystal fiber-based plasmonic biosensor: A platform for detection of coronavirus. *Biosensors and Bioelectronics,* 205, 114107.

Shen, H., Wang, Z., Wu, Y., & Yang, B. (2016). One-dimensional photonic crystals: Fabrication, responsiveness and emerging applications in 3D construction. *RSC Adv., 6*(6), *4505–4520*.

Soltani, O., Francoeur, S., & Kanzari, M. (2023). Detecting cancerous human liver cells with high performances using photonic crystals. *Physica B: Condensed Matter, 650,* 414637.

Suthar, A. B., & Bhargava, A. (2021). Biosensor application of one-dimensional photonic crystal for malaria diagnosis. *Plasmonics, 16*, 59–63.

Tan, Y., Xue, J., Zhang, W., et al. (2015). Photonic crystal hydrogel enhanced plasmonic staining for multiplexed protein analysis. *Biosensors and Bioelectronics, 74*, 425–431.

Taya, S. A., Sharma, A., Doghmosh, N., & Colak, I. (2022). Detection of water concentration in ethanol solution using a ternary photonic crystal-based sensor. *Materials Chemistry and Physics, 279,* 125786.

Thomas, S. (2023). Material applications of gelatin. In Handbook of Biopolymers. Springer Nature Singapore.

Uddin, S. M. K., Johan, M. R., Hossain, M. A. M., Sagadevan, S., & Amin, M. (2021). Halal and kosher gelatin: Applications as well as detection approaches with challenges and prospects. *Food Hydrocolloids, 44,* 101422.

Wang, F., Meng, Z., Xuen, F., Xue, M., Lu, W., Chen, W., Wang, Q., & Wang, Y. (2014). Responsive photonic crystal for the sensing of environmental pollutants. *TrAC Trends in Environmental Analytical Chemistry, 3*, 1–6.

Wei, Q., Bi, D., Qi, X., Ren, M., & Wu, F. (2025). Angle-independent topological interface states in one-dimensional photonic crystal heterostructures containing hyperbolic metamaterials. *Optics Letters, 50*(2), 451–454.

Wu, F., Chen, M., & Xiao, S. (2022). Wide-angle polarization selectivity based on anomalous defect mode in photonic crystal containing hyperbolic metamaterials. *Optics Letters, 47*(9), 2153–2156.

Wu, F., She, Y., Jiang, H., Liu, G., Chen, G., & Xiao, S. (2025). Angle-immune strong coupling between two defect modes in a defective photonic hypercrystal. *Optics and Lasers in Engineering, 186*, 108842.

Yablonovitch, E. (1987). Inhibited spontaneous emission in solid-state physics and electronics. *Physical Review Letters, 58*, 2059–2062.

Yang, Y., Xiang, Y., & Qi, X. (2023). Design of photonic crystal biosensors for cancer cell detection. *Micromachines, 14*(7), 1478

Yeh, P. (2005). Optical waves in layered media. Wiley-Interscience.

Zaky, Z. A., Sharma, A., Alamri, S., Saleh, N., & Aly, A. H. (2022). Detection of fat concentration in milk using ternary photonic crystal. *Silicon, 14*, 6063–6073.

Zhang, Y., Yu, H., Dong, J., et al. (2019). All-silicon spectrally resolved interferometric circuit for multiplexed diagnostics: A monolithic lab-on-a-chip integrating all active and passive components. *ACS Photonics, 6*(7), 1694–1705.

Zheng, S., Dong, G., & Yang, Q. (2021). Ultra-compact photonic crystal couplers for optical switches based on band-edge resonance. *Advanced Composites and Hybrid Materials, 4*, 1179–1186.

Manuscript Received: 9 February 2026
1st Manuscript Revision Received: 12 May 2026
2nd Manuscript Revision Received: 18 June 2026
Accepted Manuscript: 22 July 2026